02

Optimizing the conditions for functionalizing glass with fluorescently labeled oligonucleotides for the creation of reproducible DNA nanosensor and photonic devices

© V.V. Veselova[1], K.V. Arabuli[2], P.V. Filatov[2,¶], I.A. Reznik[2,¶], M.V. Zyuzin[2]

[1] Faculty of Biotechnology, ITMO University,
St. Petersburg, Russia
[2] School of Physics and Engineering, ITMO University,
St. Petersburg, Russia

[¶] e-mail: filatovpaul22@gmail.com, ivan.reznik@metalab.ifmo.ru

Received October 30, 2025
Revised November 19, 2025
Accepted November 20, 2025

Optimization of glass surface functionalization is a critical step in developing highly sensitive DNA nanosensors and photonic devices. In this study, a systematic comparative analysis was performed to evaluate the efficiency of four glass surface activation protocols - two chemical and two physico-chemical - in combination with different concentrations of (3-aminopropyl)triethoxysilane (APTES: 1%, 2%, and 4% v/v). For the first time, a universal molecular beacon (UMB) labeled with fluorescein (FAM) was used as the immobilized oligonucleotide. The efficiency of each method was assessed by contact angle measurements and fluorescence analysis, including the signal-to-background (S/B) ratio calculation. It was shown that oxygen plasma-based protocols produced the most hydrophilic surfaces (contact angle $4.9^\circ - 5.5^\circ$) but yielded lower S/B ratios compared to chemical activation. The best results were obtained using Protocol 1 (chemical activation with sulfuric acid and hydrogen peroxide) combined with 2% APTES, providing the highest S/B ratio (5.2 ± 0.9). Thus, the optimal protocol for UMB immobilization on glass was identified, providing a reliable foundation for the development of advanced DNA nanosensors and photonic devices.

Keywords: Glass functionalization, Oligonucleotide immobilization, DNA nanosensors, DNA photonics, Surface activation.

DOI: 10.61011/EOS.2025.11.62925.8712-25

1. Introduction

The development of nanotechnology provides the foundation for the directed design of functional materials and devices whose properties are controlled at the molecular level. In this context, nucleic acid-based technologies hold a special position due to their unique combination of characteristics, enabling their wide application. The key advantage lies in the ability to program self-assembly of structures with nanometer precision through Watson-Crick interactions [1], allowing the creation of objects with precisely defined shapes [2,3]. This molecular assembly capability underpins the development of highly specific sensor and therapeutic systems [4–6], whose effectiveness is enhanced by the high biocompatibility and biodegradability of DNA nanostructures [7–9]. An important aspect is also the ability to form heterostructures by immobilizing oligonucleotides on the surface of various materials, such as plasmonic [10] and magnetic nanoparticles [11], graphene nanostructures [12], polymers [13], and silicon dioxide [14], opening prospects for detecting single nucleotide polymorphisms, mutations, and gene expression levels.

DNA technologies also demonstrate significant potential in other interdisciplinary research areas. A promising direction is the integration of DNA technologies into photonics, enabling the creation of fundamentally new systems with unique properties. Thus, DNA can serve as a highly efficient matrix for integrating organic dyes, quantum dots, and chromophores, preventing their aggregation and enabling the creation of nonlinear optical materials with pronounced nonlinear refractive indices and two-photon absorption [15–19]. It has also been shown that stabilizing dye molecules in a DNA matrix on a glass substrate leads to a significant increase in fluorescence quantum yield due to suppression of non-radiative transitions, providing the basis for developing biocompatible waveguide lasers and highly efficient fluorescent sensors [20–22]. Incorporating DNA structures into photonic systems allows nanometer-precision spatial organization of plasmonic nanoparticles and quantum dots, enabling the design of complex devices such as plasmonic nanoantennas, waveguides, metasurfaces, and photonic crystals [23,24]. Moreover, integrating DNA sensors directly into optical waveguides forms the basis for lab-on-a-chip systems, enabling highly sensitive detection of biological analytes [25,26].

Despite the diversity of directions in DNA photonics, systems based on oligonucleotides immobilized on glass play a special role. Such systems possess a unique set of

characteristics critical for optical applications: high transparency from visible to IR radiation (400–1700 nm) [27–29], low optical losses in waveguides (on the order of 0.06 dB/cm) [30], chemical inertness and resistance to most reagents, ensuring long-term stability of immobilized structures, as well as simplicity of fabrication and low cost. These advantages make such systems an extremely promising platform for creating modern photonic and sensor systems [31–33].

A key stage in creating highly sensitive biosensors is the optimal functionalization of glass substrates with oligonucleotides, requiring the selection of appropriate chemical and physical surface properties for stable and specific binding while preserving biological activity. Surface cleaning and activation is one of the main stages ensuring uniform coating, reproducibility, and durability of the functionalized surface. Moreover, such parameters as undesirable molecular orientation and conformation, background signal, and non-specific binding can reduce sensor sensitivity and selectivity. Together, this underscores the need for comprehensive analysis and optimization of glass substrate functionalization with oligonucleotides [34].

Despite the broad applicability of methods based on oligonucleotides immobilized on glass substrates, systematic comparisons of surface modification protocols are currently lacking. This fact necessitates comprehensive experiments to select optimal protocols before starting research. In this work, multifactor optimization was conducted, examining several glass silanization protocols using (3-aminopropyl)triethoxysilane (APTES), which is one of the key modification factors. To this end, two chemical and two physical activation protocols were selected, followed by use of various APTES concentrations (1%, 2%, and 4% v/v). A universal molecular beacon (UMB) was used as the immobilized oligonucleotide. To our knowledge, UMB was immobilized on an APTES-silanized glass substrate for the first time [35]. The surface modification optimization conducted in this work lays the foundation for developing high-quality, reproducible DNA sensors and photonic devices, as it establishes a standardized and efficient surface preparation protocol that is critically important for their sensitivity and stability.

2. Materials and methods

2.1. Materials and equipment

(3-Aminopropyl)triethoxysilane/APTES (ThermoFisher Scientific, USA), microscope slides 26 x 76 mm (Minimede, Russia), ethyl alcohol (Ekos, Russia), acetone (Ekos, Russia), sodium hydroxide (Sigma-Aldrich, USA), potassium hydroxide (Sigma-Aldrich, USA), isopropyl alcohol (Ekos, Russia), chloroform (Ekos, Russia), methyl alcohol (Chimmed, Russia), glutaraldehyde (ThermoFisher Scientific, USA), phosphate-buffered saline (PBS) (Biolot, Russia), acetic acid (Ekos, Russia), oligonucleotide solution (DNA SYNTHESIS, Russia), sulfuric acid solution (Lenreaktiv, Russia), and 30% hydrogen peroxide (Aldosa, Russia) (in a 3:1 ratio). Orbital shaker Vibramax 100 (Heidolph, Germany), ultrasonic bath „Sapphire“ TTC (Sapphire, Russia), dry heat oven Binder ED 53 Avantgarde.Line (Binder GmbH, Germany), low-pressure plasma system (Diener ZEPTO 13.56 MHz, Ebhausen, Germany).

2.2. Methods

2.2.1. Glass Cleaning and Activation For oligonucleotide immobilization, the glass surface was pre-activated. Four protocols were selected for the activation process, differing in the type of treatment (chemical, physical) and number of stages.

In **Protocol 1**, slides were placed in a 40 ml Coplin staining jar half-filled with a solution of ethanol and sodium hydroxide (10 M) in a 3:7 ratio and incubated for 30 min on an orbital shaker. They were then rinsed with distilled water and dried under nitrogen atmosphere. Afterward, the slides were half-immersed in a solution of sulfuric acid and hydrogen peroxide (3:1 ratio) and incubated for 30 min on an orbital shaker. After activation, the glasses were rinsed with distilled water and dried under nitrogen atmosphere [36].

Using **Protocol 2**, slides half-immersed in acetone were treated in an ultrasonic bath for 30 min at 30 °C. They were then rinsed with distilled water and subjected to ultrasonic treatment in 5 M KOH solution for 45 min at 30 °C. The glasses were then rinsed with distilled water and subjected to ultrasonic treatment for 10 min at 30 °C. Afterward, the glasses were rinsed again with distilled water and acetone and dried under nitrogen atmosphere. hey were then placed in a dry heat oven at 110 °C for 30 min. After drying, the slides were cleaned in oxygen plasma for 10 min at 80% power [37].

In **Protocol 3**, slides were sequentially activated for 30 s with chloroform, isopropyl alcohol, methanol, and distilled water, then dried under nitrogen atmosphere [28].

For activation according to **Protocol 4**, slides half-immersed in acetone were incubated in an ultrasonic bath for 10 min, then acetone was replaced with isopropyl alcohol and incubated in the ultrasonic bath for another 10 min. The same steps were repeated, and after cleaning with isopropyl alcohol, the glasses were dried at room temperature. After drying, the slides were treated in oxygen plasma for 5 min at 80% power [38].

2.2.2. Contact Angle Measurement After performing the activation protocols on control slides, the water contact angle was measured using an OCA 15EC instrument (Filderstadt, Germany). Using the SD-DM direct dosing system combined with an ES electronic dosing module, drops of distilled water 10 μl were applied to the slides and captured using a USB camera. Numerical contact angle values were obtained by processing the data with SCA 20 software.

2.2.3. Glass Modification Within 5 min after activation, the glasses were placed in trays half-filled with various APTES concentrations (1%, 2%, and 4% v/v) in ethyl alcohol for 2 h at room temperature. After incubation, the slides were rinsed with 96% ethanol, 6% acetic acid, and ethanol again for 5 min each on an orbital shaker. The resulting glass samples were then placed in a dry heat oven for 20 min at 150 °C [39].

The glasses were then immersed in a 2.5% glutaraldehyde solution in 1X PBS for 1.5 h at room temperature in the dark. After incubation, the slides were rinsed with distilled water, 1X PBS, and water again for 5 min each on an orbital shaker. They were then dried at room temperature.

After drying, 10 μM oligonucleotide solution was applied to the prepared glasses in a volume of 20 μl, as a control, buffer without oligonucleotides was applied in the same volume. The glasses with oligonucleotides were incubated for 2.5 h at room temperature in humidity-controlled containers protected from light. The slides were then rinsed with distilled water, 10X PBS, and water again for 5 min each on an orbital shaker. The glasses were then placed vertically and dried at room temperature. After drying, buffer (Tris 7.4 and 50 mM $MgCl_2$) was applied to the areas where the oligonucleotide solution had previously been deposited and incubated for 20 min at room temperature.

2.2.4. Fluorescence Signal Readout For fluorescence readout, a fluorimetric optical setup (Fig. S1, Supplementary Information) was assembled based on the double monochromator principle to ensure high spectral selectivity and background suppression. A halogen lamp Avantes served as the excitation light source. The lamp emission passed through an entrance rectangular slit 50 μm wide, which formed a narrow, well-collimated light beam. The light then reached an entrance reflective blazed diffraction grating with a groove density of 1200 mm^{-1} designed for spectral dispersion of the input radiation and selection of the required excitation wavelength (493 nm). The diffracted light was directed via silver mirrors to the sample with immobilized oligonucleotides. The emitted radiation was directed to an exit diffraction grating similar in parameters to the entrance grating. This grating separated scattered light and background radiation while selecting emission in a narrow spectral range around 517 nm, which was focused on a photomultiplier tube.

3. Results

This work conducted a comparative study of two main directions for glass surface activation: physico-chemical and chemical methods. The physico-chemical approach was represented by Protocols 2 and 4, based on oxygen plasma treatment but differing in glass pre-treatment methodology (see section 2.2.1). In **Protocol 2**, cleaning with organic and alkaline solvents, combined with ultrasonication and oven incubation, activated the glass surface and removed all contaminants before oxygen plasma treatment. In contrast, Protocol 4 used only organic solvents and shorter treatment times before plasma cleaning compared to Protocol 2. Chemical activation methods included **Protocol 1** using alkali and a sulfuric acid/hydrogen peroxide solution, and the milder **Protocol 3** based on organic solvents. The protocol diagrams are shown in Fig. 1.

3.1. Contact Angle Measurement of Activated Glass Surface

To initially validate the efficiency of the selected activation protocols, contact angle measurements were performed to quantitatively assess the hydrophilic-hydrophobic properties of the glass surfaces. A schematic representation of the measurement method is shown in Fig. 2, *a*. Analysis of the obtained data demonstrated substantial differences in surface wettability depending on the activation protocol used. The lowest contact angle value, indicating maximum surface hydrophilicity, was recorded for **Protocol 2** at $4.9 \pm 0.8°$. Similar hydrophilicity was shown by **Protocol 4** ($5.5 \pm 0.3°$). **Protocol 1** provided contact angle values of $10.3 \pm 1.5°$, while **Protocol 3** resulted in the most hydrophobic surface with a contact angle of $22.7 \pm 2.4°$. Non-activated glass surface was used as a control with a contact angle of $29.0 \pm 5.5°$. This confirms the effectiveness of all activation protocols in increasing surface hydrophilicity.

The studies showed that surfaces treated with oxygen plasma exhibited the greatest hydrophilicity, consistent with literature data [40]. This high hydrophilicity is explained by the formation of hydroxyl groups (Si−OH) and siloxane bonds (Si−O−Si), on the glass surface, imparting superhydrophilic properties and increased reactivity [41,42]. However, this method has a significant limitation: studies show that the high reactivity of the plasma-treated surface persists for only a few minutes after treatment, after which polar groups undergo recombination or adsorb airborne contaminants, substantially losing their reactivity [43]. Additionally, this method requires expensive equipment.

The chemical method based on immersion treatment of glass is widely used in cleaning and subsequent silanization protocols to obtain uniformly functionalized surfaces. It ensures uniform reagent-surface contact, leading to homogeneous distribution of reactive groups. However, factors such as fluid dynamics, temperature gradients, and surface micro-roughness can cause local variations in reagent concentration and reaction kinetics [44]. To minimize these effects, shakers or ultrasonication should be used, which improve mass transfer and ensure cleaning uniformity across the entire surface.

Most commonly, a sulfuric acid and hydrogen peroxide solution (piranha solution) is used for chemical cleaning. Its distinctive feature is the ability to hydrolyze siloxane bonds (Si−O−Si) on the surface, regenerating silanol groups (Si−OH), which significantly increases surface hydrophilicity [45].

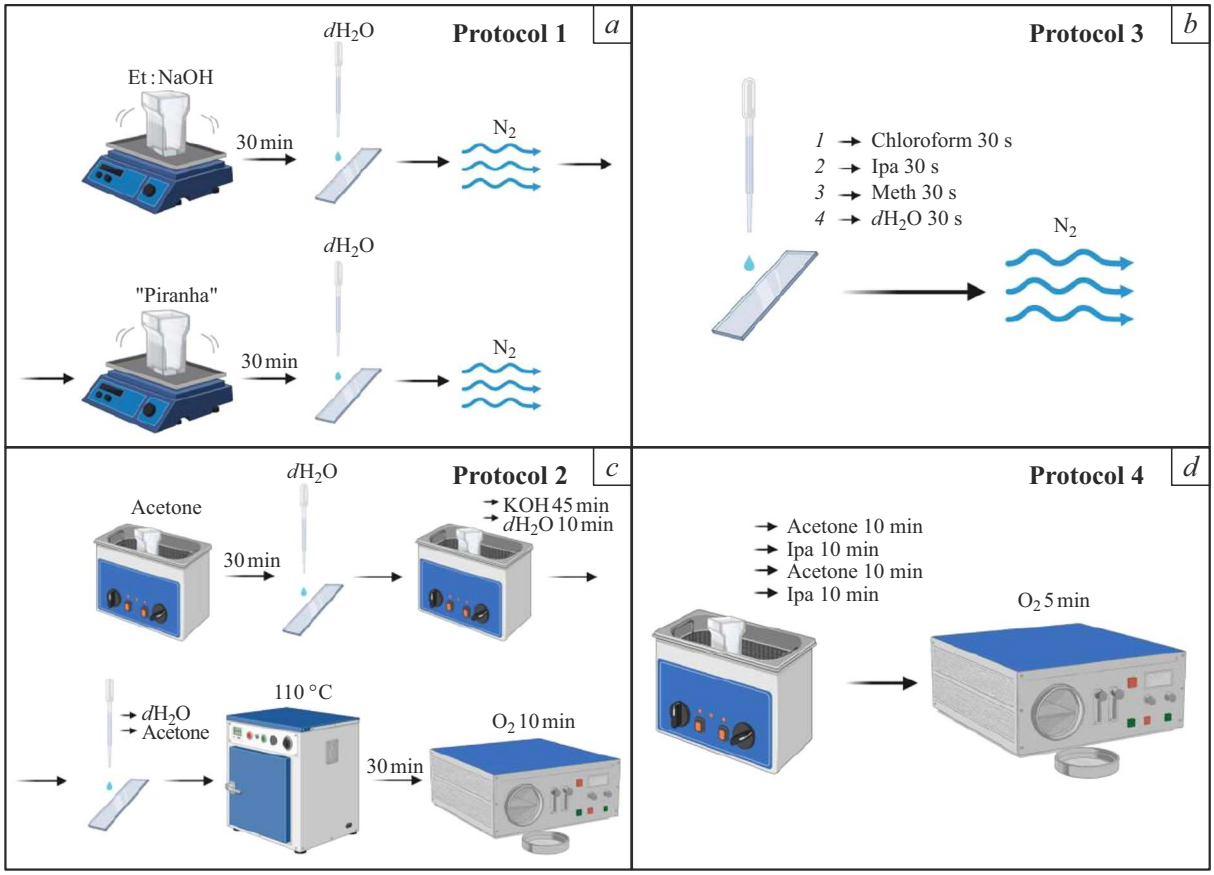

Figure 1. Schematic diagrams of glass surface activation protocols: chemica — **Protocol 1** (*a*), **Protocol 3** (*b*) and physico-chemical — **Protocol 2** (c) and **Protocol 4** (*d*).

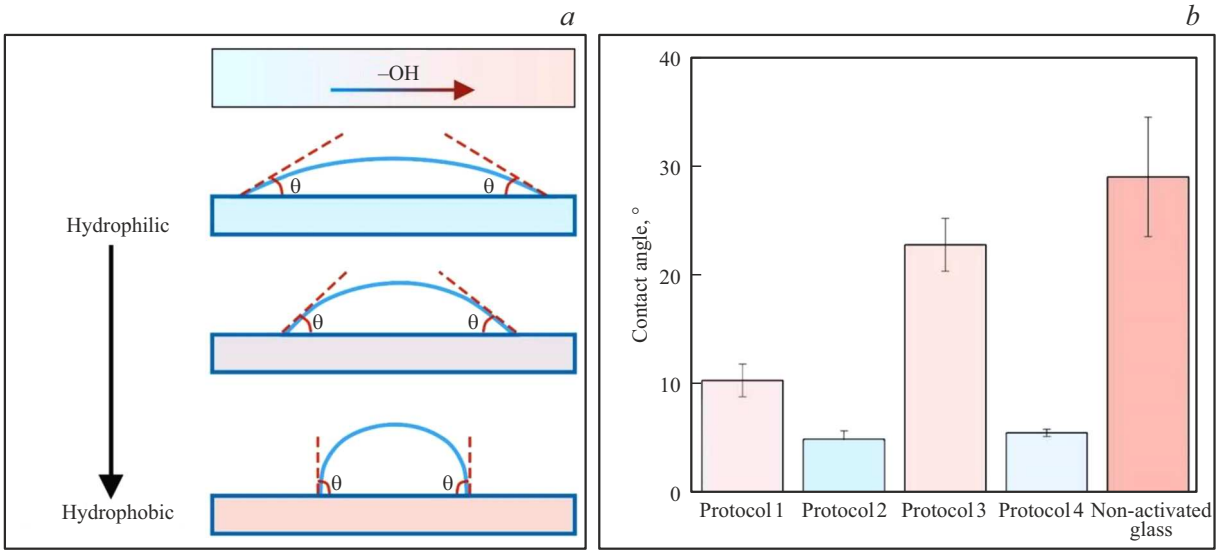

Figure 2. Contact angle measurement: (*a*) Schematic diagram of the method principle with color coding showing the relationship between the number of hydroxyl groups (−OH) on the surface and the contact angle θ: blue corresponds to hydrophilic surfaces with a large number of −OH-groups and low θ values, red — to hydrophobic surfaces with fewer OH groups and higher θ values. (*b*) Contact angle values for surfaces cleaned and activated by different protocols (**Protocols 1**−**4**), as well as for non-activated glass (Non-activated Glass).

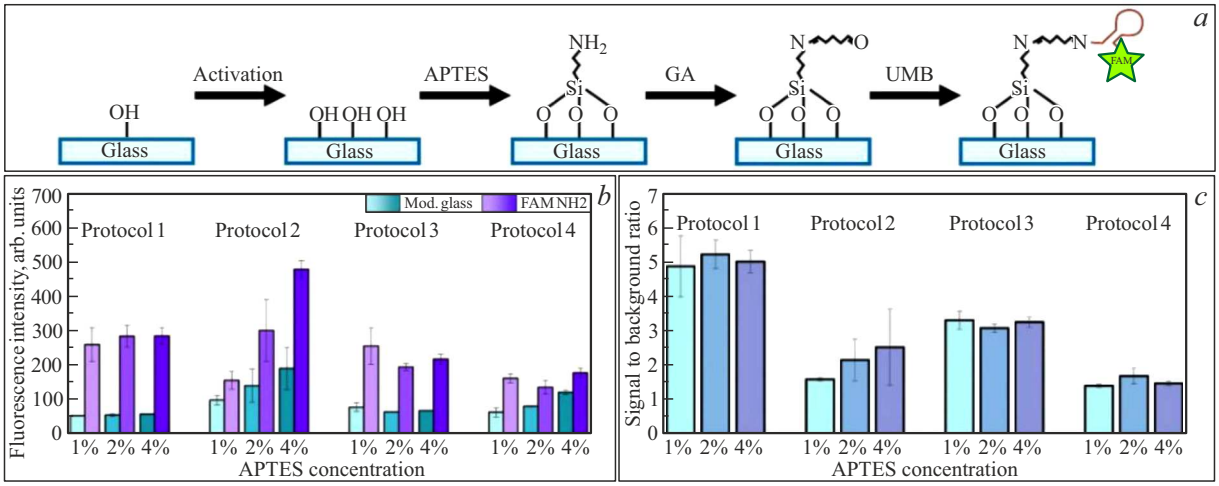

Figure 3. Experimental scheme (*a*). Fluorescence intensity values for glasses treated by different activation protocols using 1%, 2%, and 4% APTES concentrations (*b*). Signals from target zones with immobilized FAM-labeled UMB (FAM NH_2) were compared to control zones without oligonucleotides (Mod. Glass). Calculated signal-to-background (S/B) ratios for all studied conditions (*c*).

Meanwhile, for glass with a high initial content of silanol groups, cleaning with organic solvents may suffice to effectively remove surface contaminants. Importantly, unlike piranha solution treatment, immersion in organic solvents does not increase the density of silanol (Si−OH) or other polar groups on the glass surface but merely exposes existing hydroxyl centers by removing organic contaminants that block their reactivity. This is confirmed by our results showing that glass hydrophilicity before and after organic solvent cleaning differs insignificantly (after **Protocol 4** $22.7 \pm 2.4°$, pristine glass $28.95 \pm 5.5°$), indicating preservation of the initial silanol group density.

3.2. Fluorescence Analysis of Surfaces Using Labeled Oligonucleotides

To confirm successful oligonucleotide immobilization and assess non-specific adsorption levels after hydrophilicity analysis, fluorescence measurements were performed using the assembled optical setup (Fig. S1). Fluorescence signal intensity was compared between target zones (glass modified with FAM-labeled UMB oligonucleotide with NH_2 group) and control zones (glass after APTES+GA modification without oligonucleotides). The overall experimental diagram is shown in Fig. 3, *a*.

The results showed that for **Protocol 1**, fluorescence levels at different APTES concentrations remained relatively stable, varying in target zones from 260.5 ± 49.9 at 2% APTES) to 285.7 ± 24.7 arb. units (at 4% APTES). Control zone signals were 53.0 ± 1.1, 54.6 ± 3.4, 57.0 ± 1.2 arb. units for 1%, 2%, and 4%, respectively. For **Protocol 2**, a clear dependence of fluorescence intensity on APTES concentration was observed: target zone values increased from 155.8 ± 25.7 (1%) to 480.2 ± 24.7 arb. units (4%), while control zone growth was less pronounced, from 98.2 ± 13.9 to 190.7 ± 61.8 arb. units. For **Protocol 3**, maximum target zone fluorescence was recorded at 1% APTES 1% (256.4 ± 53.7 arb. units), decreasing at 2% and 4% to 195.0 ± 10.1 and 217.7 ± 14.2 arb. units respectively. Control zones showed a similar trend: 77.8 ± 12.8 (1%), 63.5 ± 0.9 (2%) and 67.1 ± 1.4 arb. units (4%). For **Protocol 4**, target zone fluorescence values were 161.9 ± 12.8 (1%), 135.9 ± 19.8 (2%) and 177.8 ± 14.0 arb. units (4%), while control zones showed 115.6 ± 13.2, 80.8 ± 1.6 and 121.0 ± 6.8 arb. units for the respective APTES concentrations (Fig. 3, *b*).

Subsequent signal-to-background (S/B) ratio calculations revealed that the highest values were achieved using **Protocol 1**. The maximum S/B ratio was demonstrated by samples with 2% APTES (5.2 ± 0.9). For other concentrations within this protocol, similar values were obtained: 4.9 ± 0.9 for 1% and 5.0 ± 0.3 for 4% APTES (Fig. 3, *c*). For **Protocol 2**, the highest S/B was 2.5 ± 1.1 at 4% APTES; for **Protocol 3** — 3.3 ± 0.3at 1% APTES; for **Protocol 4** — 1.7 ± 0.2 at 2% APTES.

The key criterion for evaluating immobilization method efficiency is the signal-to-background (S/B) ratio, which is of primary importance for most practical applications. This parameter is more informative than absolute fluorescence values, as it reflects not only the specific signal level from the target zone with fluorophore-labeled immobilized oligonucleotides but also the background signal intensity from the control zone. This aspect is particularly important in the context of the surface modification chemistry used, where sequential application of amine-containing APTES and aldehyde-containing GA leads to Schiff base formation with intrinsic fluorescence [46]. Thus, a high background signal indicates intense uncontrolled Schiff base formation, which may result from extended APTES-based polymeric structures and suggests insufficient reproducibility of surface modification results.

It is also important to note in the context of this study that UMB — a molecular beacon serving as a molecular foundation for DNA construct assembly on the surface — was used as the immobilized oligonucleotide. This sequence forms a stable hairpin structure without sequences capable of unfolding it into a linear configuration [47]. This architecture provides a convenient tool for DNA construct immobilization, as previously confirmed in creating ultraspecific DNA sensors [31,35,48]. However, literature primarily reports electrochemical detection with UMB immobilization on gold substrates, while UMB immobilization on glass surfaces remains a promising and underexplored scientific challenge.

4. Conclusions

This study conducted a comprehensive comparative analysis of glass surface activation methods for subsequent DNA structure immobilization. The research aimed at systematically evaluating the efficiency of various activation and surface modification protocols to identify the optimal method for creating functional surfaces in DNA photonics.

A comparison was made between two main activation approaches: physico-chemical methods (**Protocols 2** and **3** based on oxygen plasma) and chemical methods (**Protocol 1** with sulfuric acid/hydrogen peroxide solution and **Protocol 4** with organic solvents). Surface hydrophilicity analysis showed that oxygen plasma-treated surfaces exhibited the greatest hydrophilicity (**Protocol 2**: $4.9 \pm 0.8°$; **Protocol 4**: $5.5 \pm 0.3°$), however, these methods have limitations related to temporal instability of the activated surface and the need for expensive equipment.

Fluorescence analysis using FAM-labeled UMB oligonucleotides demonstrated that the best results were achieved with **Protocol 1** at 2% APTES concentration, which showed the maximum signal-to-background ratio (5.2 ± 0.9). This protocol ensures stable target zone fluorescence values (260.5 ± 49.9 arb. units at 2% APTES to 285.7 ± 24.7 arb. units at 4% APTES) with minimal background signal (53.0−57.0 arb. units), indicating a controlled immobilization process and absence of non-specific adsorption.

Thus, **Protocol 1** with 2% APTES concentration was identified as the optimal method for preparing glass surfaces for DNA structure immobilization, providing a high signal-to-background ratio and reproducible results, making it promising for applications in DNA photonics and sensor systems.

Funding

This research was supported by the Russian Science Foundation grant № 25-73-20100.

Conflict of interest

The authors declare that they have no conflict of interest.

References

[1] C. Zhou, Y. Song, X. Jin, B. Li, C. Pang. Nanoscale Horiz, **8**, 176 (2023). DOI: 10.1039/D2NH00525E
[2] S. Julin, S. Nummelin, M.A. Kostiainen, V. Linko. J. Nanoparticle Res., **20**, 119 (2018). DOI: 10.1007/s11051-018-4225-3
[3] T. Tian, Y. Li, Y. Lin. Bone Res., **10**, 40 (2022). DOI: 10.1038/s41413-022-00212-1

Appendix

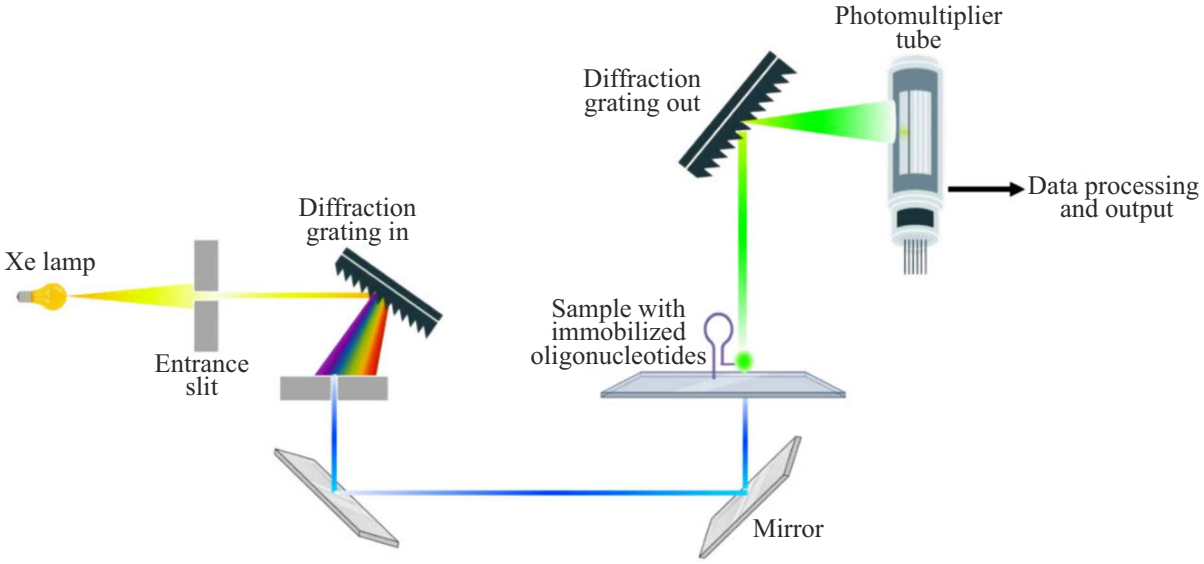

Fig. S1. Optical scheme of the monochromator for fluorescence measurement.

[4] J. Zhou, J. Rossi. Nat. Rev. Drug Discov., **16**, 181 (2017). DOI: 10.1038/nrd.2016.199
[5] Z. Suo, J. Chen, X. Hou, Z. Hu, F. Xing, L. Feng. RSC Adv., **9**, 16479 (2019). DOI: 10.1039/C9RA01261C
[6] H. Wang, H. Zou, F. Wang, ChemBioChem, **25**, e202400266 (2024). DOI: 10.1002/cbic.202400266
[7] S. Ghosal, S. Bag, S. Bhowmik, Polymers, **15**, (2023). DOI: 10.3390/polym15081850
[8] X. Huang, N.T. Blum, J. Lin, J. Shi, C. Zhang, P. Huang, Mater Horiz, **8**, 78 (2021). DOI: 10.1039/D0MH00715C
[9] J. Huang, A. Chakraborty, L.S. Tadepalli, A. Paul, ACS Pharmacol. Transl. Sci., **7**, 2204 (2024). DOI: 10.1021/acsptsci.4c00308
[10] C.S. Huertas, M. Soler, M.-C. Estevez, L.M. Lechuga, Anal. Chem., **92**, 12596 (2020). DOI: 10.1021/acs.analchem.0c02619
[11] A. Ligasová, I. Rosenberg, M. Bockov., J. Homola, K. Koberna, Open Biol., **11**, 210136 (2021). DOI: 10.1098/rsob.210136
[12] F. Gao, X. Cai, H. Tanaka, Q. Zhu, F. Gao, Q. Wang. J. Electrochem. Soc., **162**, B291 (2015). DOI: 10.1149/2.0011512jes
[13] D.K. Kannoujia, S. Ali, P. Nahar. Anal Methods, **2**, 212 (2010). DOI: 10.1039/C001661F
[14] T. Strother, R.J. Hamers, L.M. Smith. Nucleic Acids Res., **28**, 3535 (2000). DOI: 10.1093/nar/28.18.3535
[15] E.M. Heckman, J.G. Grote, P.P. Yaney, F.K. Hopkins. Nonlinear Opt. Transm. Multiphoton Process. Org. II. Ed. by A.T. Yeates (SPIE, 2004), p. 47–51. DOI: 10.1117/12.563071
[16] S. Sreeja, B. Nityaja, D. Swain, V.P.N. Nampoori, P. Radhakrishnan, S.V. Rao. Opt. Photonics J., **02**, 135 (2012). DOI: 10.4236/opj.2012.23019
[17] V. Arasu, S.R. Dugasani, M.R. Kesama, H.K. Chung, S.H. Park. Sci. Rep., **7**, 11567 (2017). DOI: 10.1038/s41598-017-11797-7
[18] A. Hajda, R. Guha, S.M. Copp, J. Olesiak-Bańska. Chem. Sci., **16**, 1737 (2025). DOI: 10.1039/D4SC05853D
[19] K. Wu, C. Ma, Y. Wang. Biosensors **13**, (2023). DOI: 10.3390/bios13090836
[20] V. Glembockyte, L. Grabenhorst, K. Trofymchuk, P. Tinnefeld. Acc. Chem. Res., **54**, 3338 (2021). DOI: 10.1021/acs.accounts.1c00307
[21] J. Malicka, I. Gryczynski, J. Fang, J.R. Lakowicz. Anal. Biochem., **317**, 136 (2003) DOI: 10.1016/S0003-2697(03)00005-8
[22] R. Khazaeinezhad, S. Hosseinzadeh Kassani, B. Paulson, H. Jeong, J. Gwak, F. Rotermund, D.-I. Yeom, K. Oh. Sci. Rep., **7**, 41480 (2017). DOI: 10.1038/srep41480
[23] A. Kuzyk, R. Jungmann, G.P. Acuna, N. Liu. ACS Photonics, **5**, 1151 (2018) DOI: 10.1021/acsphotonics.7b01580
[24] I.V. Martynenko, E. Erber, V. Ruider, M. Dass, G. Posnjak, X. Yin, P. Altpeter, T. Liedl. Nat. Nanotechnol., **18**, 1456 (2023) DOI: 10.1038/s41565-023-01487-z
[25] L. Liu, X. Zhou, J.S. Wilkinson, P. Hua, B. Song, H. Shi. Sci. Rep., **7**, 3655 (2017) DOI: 10.1038/s41598-017-03939-8
[26] I. Titov, N. Rutschke, F.A. Kraft, M. Köpke, E. Nebling, M. Gerken, Biomed Opt Express, **13**, 6300 (2022). DOI: 10.1364/BOE.475358
[27] H. Schröder, J. Schwietering, G. Böttger, V. Zamora. J. Opt. Microsyst. **1**, 033501 (2021). DOI: 10.1117/1.JOM.1.3.033501
[28] H.A. Ki, M.J. Kim, S. Pal, J.M. Song. J. Pharm. Biomed. Anal., **49**, 562 (2009). DOI: 10.1016/j.jpba.2008.11.031
[29] J. Li, H. Wang, Y. Zhao, L. Cheng, N. He, Z. Lu. Sensors, **1**, 53 (2001). DOI: 10.3390/s10100053
[30] G.C. Righini, A. Chiappini, Opt. Eng., **53**, 071819 (2014). DOI: 10.1117/1.OE.53.7.071819
[31] A. Camposeo, P. Del Carro, L. Persano, K. Cyprych, A. Szukalski, L. Sznitko, J. Mysliwiec, D. Pisignano. ACS Nano, **8**, 10893 (2014). DOI: 10.1021/nn504720b
[32] L. Ding, B. Liu, A. Peil, S. Fan, J. Chao, N. Liu, Adv. Mater. 2500086 (Early view) DOI: 10.1002/adma.202500086
[33] C.R. Sabanayagam, J.R. Lakowicz. Nucleic Acids Res. **35**, e13 (2006). DOI: 10.1093/nar/gkl1054
[34] J. Sobek, C. Aquino, R. Schlapbach. Microarrays Vol. 2 Appl. Data Anal., ed. by J.B. Rampal (Humana Press, Totowa, NJ, 2007), p. 53–66. DOI: 10.1007/978-1-59745-304-2_4
[35] D.M. Mills, M.V. Foguel, C.P. Martin, T.T. Trieu, O. Kamar, P. Calvo-Marzal, D.M. Kolpashchikov, K.Y. Chumbimuni-Torres. Sens. Actuators B Chem., **293**, 11 (2019). DOI: 10.1016/j.snb.2019.04.149
[36] A.R. Yadav, R. Sriram, J.A. Carter, B.L. Miller. Mater. Sci. Eng. C, **35**, 283 (2014). DOI: 10.1016/j.msec.2013.11.017
[37] Ł. Syga, D. Spakman, C.M. Punter, B. Poolman. Sci. Rep. **8**, 13789 (2018). DOI: 10.1038/s41598-018-32166-y
[38] M. Castano-Alvarez, D.F.P. Ayuso, M.G. Granda, M.T. Fernández-Abedul, J.R. García, A. Costa-García. Sens. Actuators B: Chem., **130** (1), 436–448 (2008) DOI: 10.1016/j.snb.2007.09.043
[39] M. Sypabekova, A. Hagemann, D. Rho, S. Kim. Biosensors **13**, (2023). DOI: 10.3390/bios13010036
[40] W.F. Paxton, P.T. McAninch, S.H.R. Shin, M.T. Brumbach. Soft Matter, **14**, 8112 (2018). DOI: 10.1039/C8SM00343B
[41] A.U. Alam, M.M.R. Howlader, M.J. Deen. ECS J. Solid State Sci. Technol., **2**, P515 (2013). DOI: 10.1149/2.007312jss
[42] A.U. Alam, M. Howlader, M.J. Deen. J. Micromechanics Microengineering, **24**, 035010 (2014). DOI: 10.1088/0960-1317/24/3/035010
[43] K. Shoda, M. Tanaka, K. Mino, Y. Kazoe, Micromachines, **11**, 804 (2020) DOI: 10.3390/mi11090804
[44] F. Lamberti, C. Luni, A. Zambon, P. Andrea Serra, M. Giomo, N. Elvassore, Biomicrofluidics, **6** (2), (2012). DOI: 10.1063/1.4705368
[45] Y. Liao, X. Chen, Y. Jiang, C. Qu, X. Liu, A. Zhao, P. Yang, N. Huang. J. Chen. Front. Bioeng. Biotechnol., **11**, 1166334 (2023). DOI: 10.3389/fbioe.2023.1166334
[46] A. Afrin, A. Jayaraj, M.S. Gayathri, Chinna Ayya Swamy P. Sensors and Diagnostics, **2**, 988 (2023). DOI: 10.1039/D3SD00110E
[47] A. Lake, S. Shang, D.M. Kolpashchikov. Angew. Chem. Int. Ed., **49**, 4459 (2010). DOI: 10.1002/anie.200907135
[48] S.-C. Sun, H.-Y. Dou, M.-C. Chuang, D.M. Kolpashchikov. Sens. Actuators B Chem., **287**, 569 (2019). DOI: 10.1016/j.snb.2019.02.073

Translated by J.Savelyeva